

Electronic Supplementary Information

Vivid-colored silicon solar panels with high efficiency and non-iridescent appearance

Chengang Ji^a, Zhong Zhang^a, Taizo Masuda^b, Yuki Kudo^b, and L. Jay Guo^{a,*}

^aDepartment of Electrical Engineering and Computer Science, The University of Michigan, Ann Arbor, Michigan 48109, USA

^bX-Frontier division, Toyota Motor Corporation, Susono-shi, Shizuoka, 471-8571, Japan

* Corresponding author: guo@umich.edu

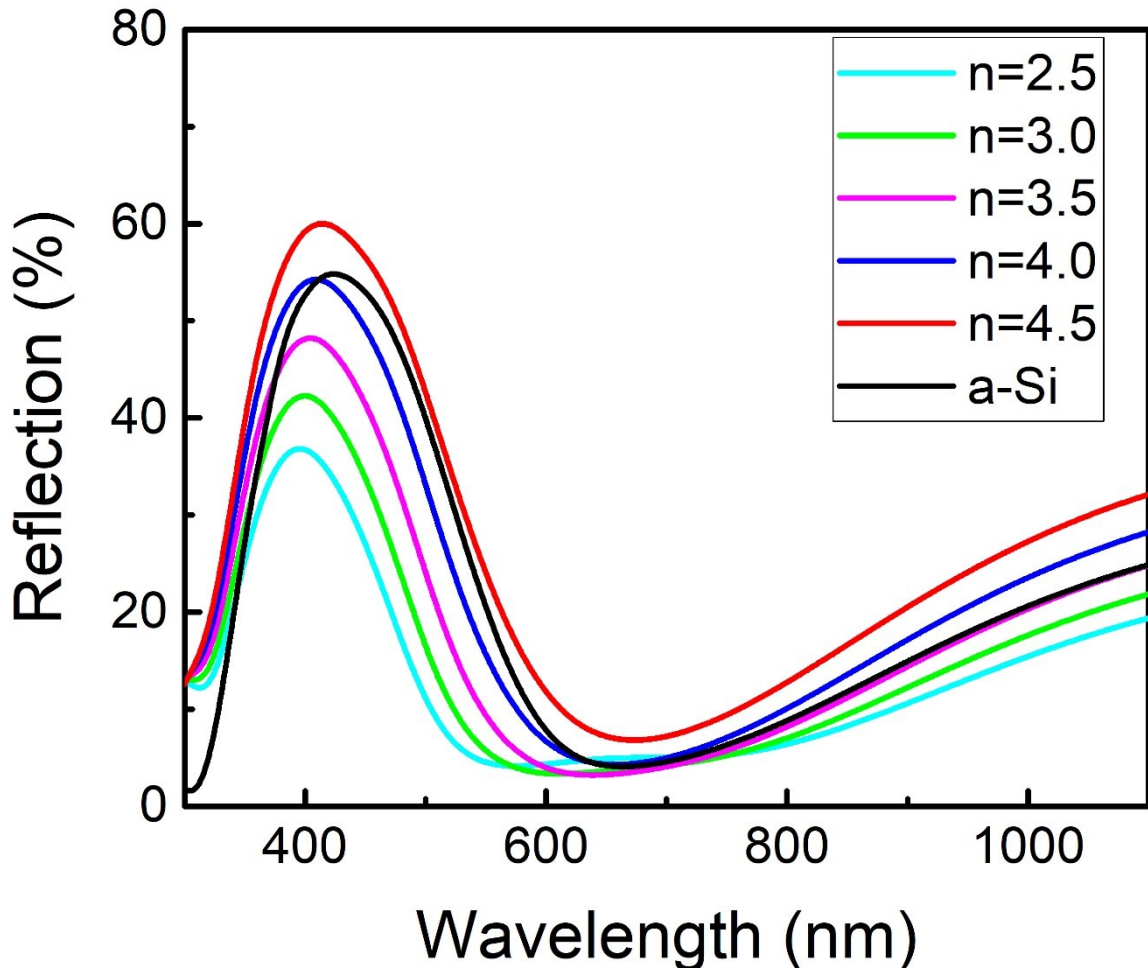


Fig. S1. Reflection spectra of blue colored structures with the middle a-Si layer replaced by materials of different refractive indices. The thicknesses of all 5 layers remain the same in each case. We have ignored the dispersion of all those materials except a-Si ($n = 4.89 + i1.28$, peak intensity $\sim 55\%$ @424 nm). As can be seen from the plot, the peak reflection intensity remains in the blue color range and increases with the refractive index: $\sim 37\%$ @397 nm ($n=2.5$), $\sim 42\%$ @400 nm ($n=3.0$), 48% @404 nm ($n=3.5$), 54% @409 nm ($n=4.0$), 60% @414 nm ($n=4.5$), thus validating that the high reflection is due to the high index of the middle layer as clarified in the main text. It is worthwhile noting that the structure employing a-Si as the middle layer does not present the highest reflection due to the material absorption at the short wavelengths although a-Si has the largest real part refractive index.

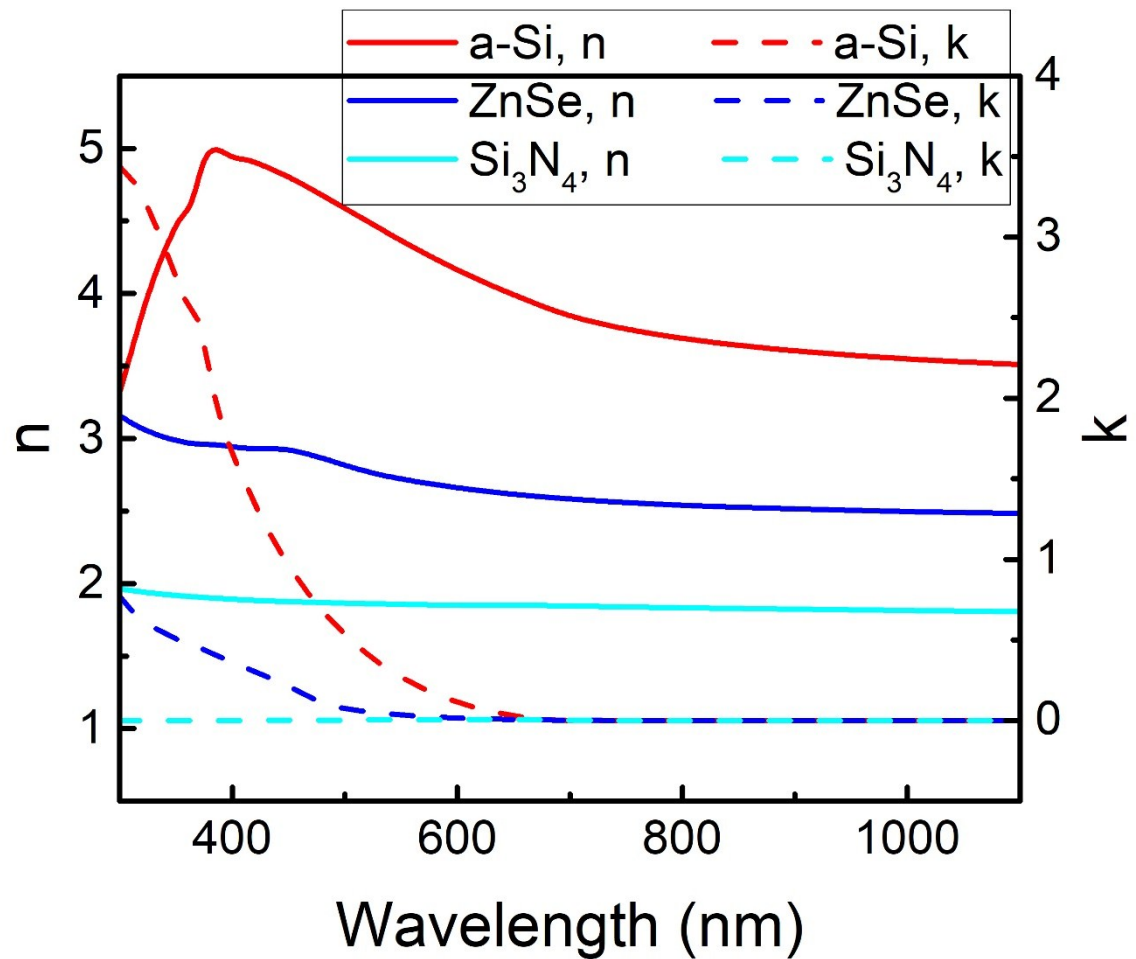


Fig. S2. Measured refractive indices of a-Si, ZnSe, and Si_3N_4 using a spectroscopic ellipsometer (M-2000, J. A. Woollam).

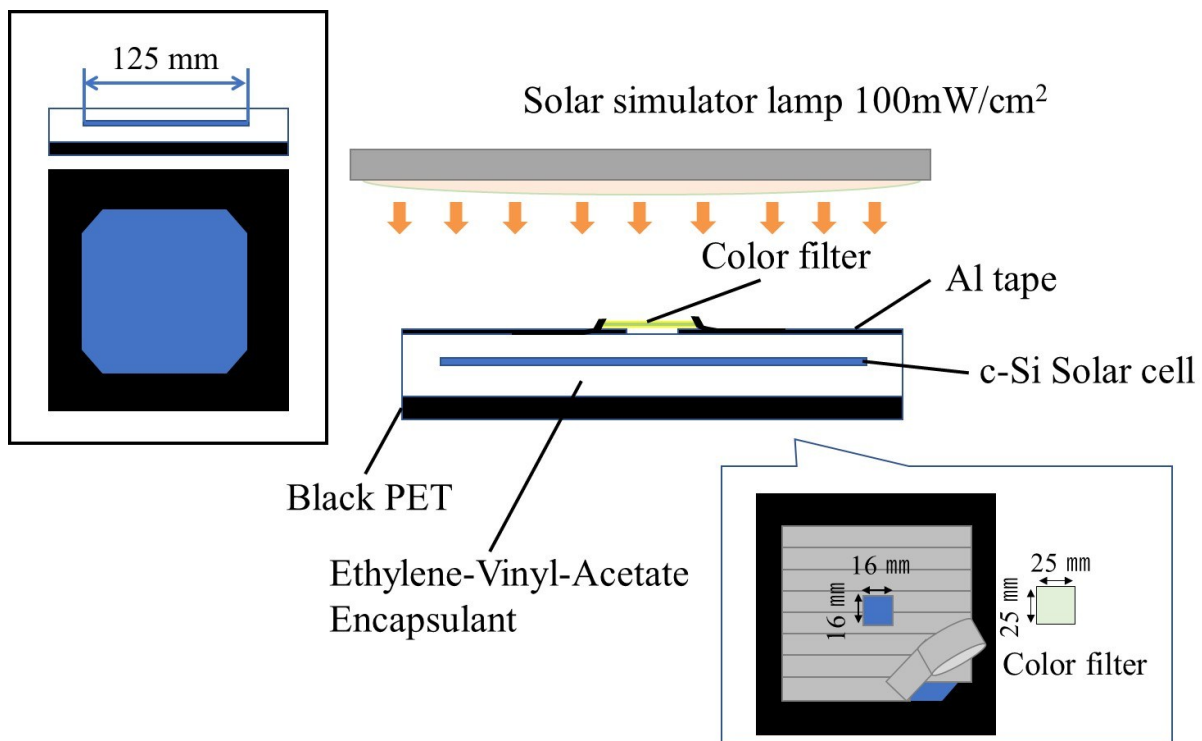


Fig. S3. Setup for the current density-voltage (J-V) data acquisition of the integrated solar cells. Insets at the top left and bottom right present the dimensions of the c-Si solar panel and aluminum (Al) tape opening at the top surface, respectively.

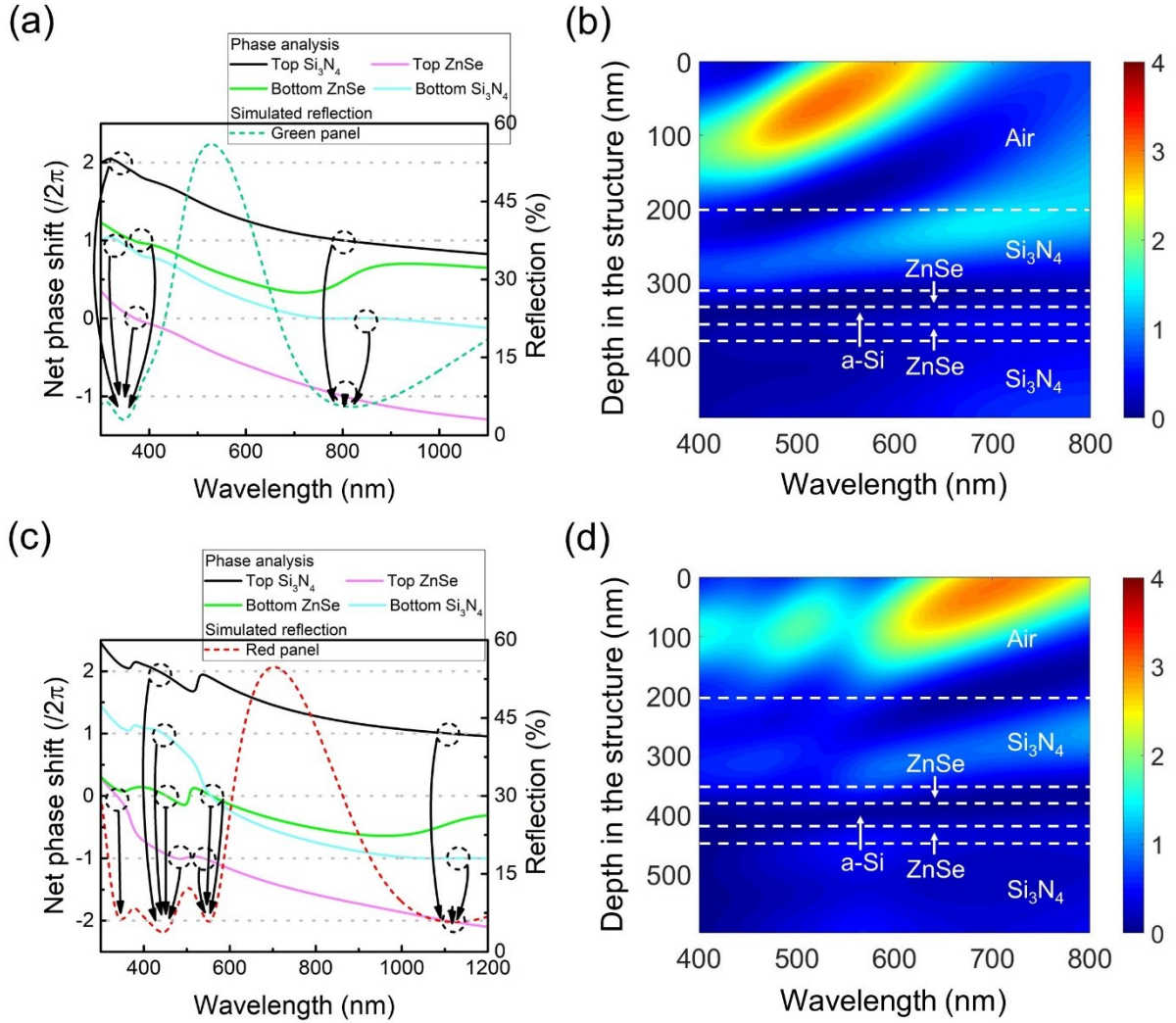


Fig. S4. (a) The calculated net phase shift, which includes the two reflection phase shifts and the propagation phase shift, inside each dielectric layer of the green color device. The transmission gets effectively enhanced at the resonances when the net phase shift is equal to a multiple of 2π . (b) The electric field distribution as functions of wavelength and depth inside the green colored device. The strong reflection in green color range (i.e., from 500 to 600 nm) unveils the reason of the distinctive colored appearance. (c) The calculated net phase shift inside each dielectric layer of the red color device. (d) The electric field distribution as functions of wavelength and depth inside the red colored device. The strong reflection at wavelengths beyond 600 nm is well consistent with the red reflection.

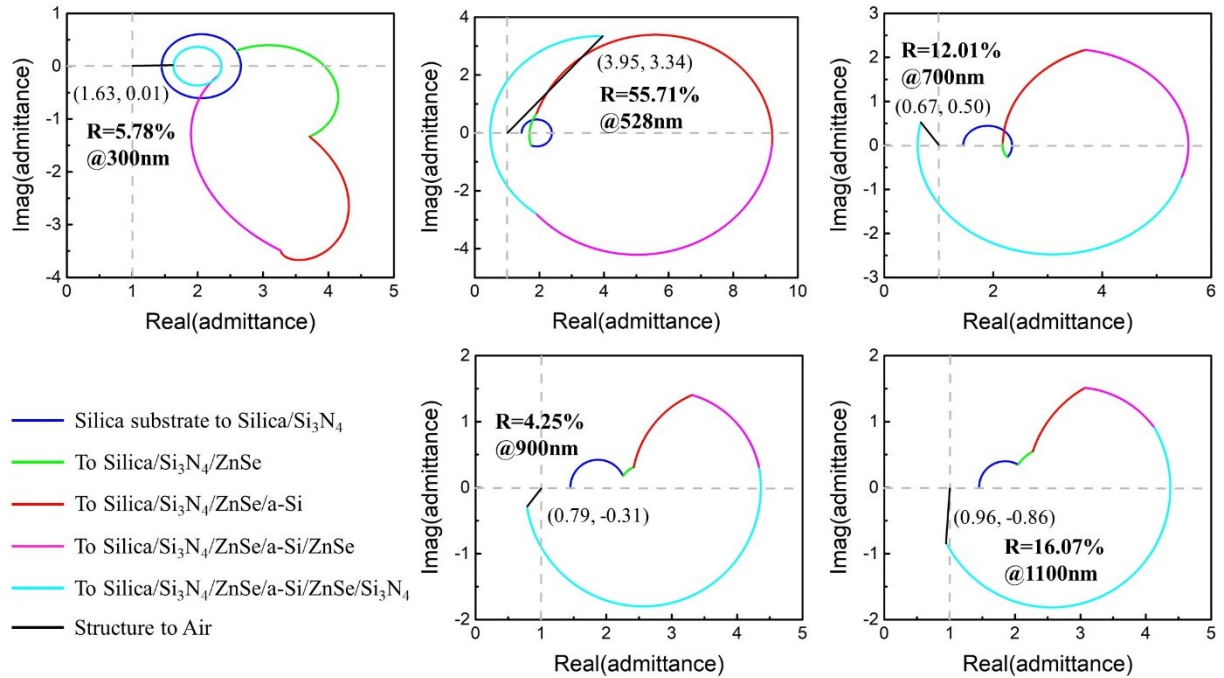


Fig. S5. Optical admittance diagrams of the green filter at 300 nm, 528 nm (reflection peak), 700 nm, 900 nm, and 1100 nm wavelengths, respectively. The reflection of the structure can be quantified with the length of the black line connecting the termination admittance point of the structure and air. The only reflection in the green color range indicates the pure colored reflection and broadband transmission of the designed device.

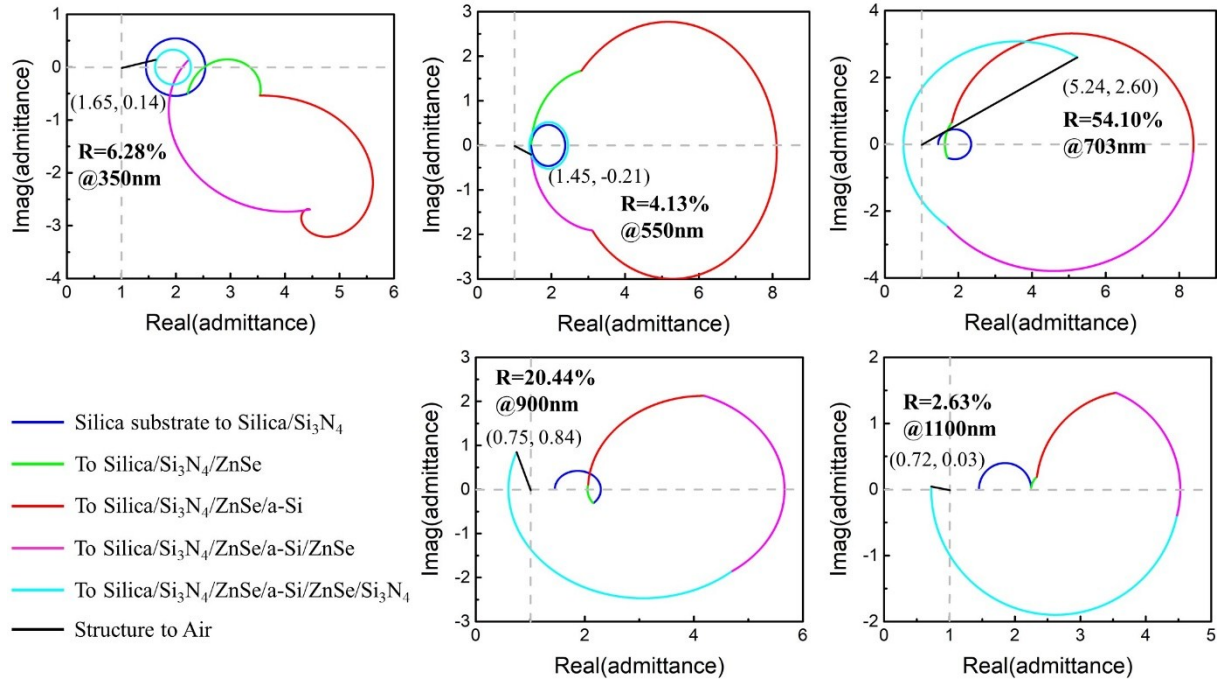


Fig. S6. Optical admittance diagrams of the red filter at 350 nm, 550 nm, 703 nm (reflection peak), 900 nm, and 1100 nm wavelengths, respectively. The reflection of the structure can be quantified with the length of the black line connecting the termination admittance point of the structure and air. The only reflection in the red color range indicates the pure colored reflection and broadband transmission of the designed device.